High-order multiscale discontinuous Galerkin methods for the one-dimensional stationary Schrödinger equation

Bo Dong

Department of Mathematics

University of Massachusetts Dartmouth

Joint work with Wei Wang (Florida International Univ.) and Chi-Wang Shu (Brown Univ.)

Partially supported by NSF and DOE

BIRS Workshop: Women In Numerical Methods for PDEs and their Applications, May 14, 2019

outline

- Model problem
- Multiscale discontinuous Galerkin (DG) methods
  - a second-order multiscale DG
  - two classes of higher order multiscale DG
- Numerical results
- Concluding Remarks

Application: modeling of quantum transport in nanoscale semiconductors

Resonant Tunneling Diode (RTD):

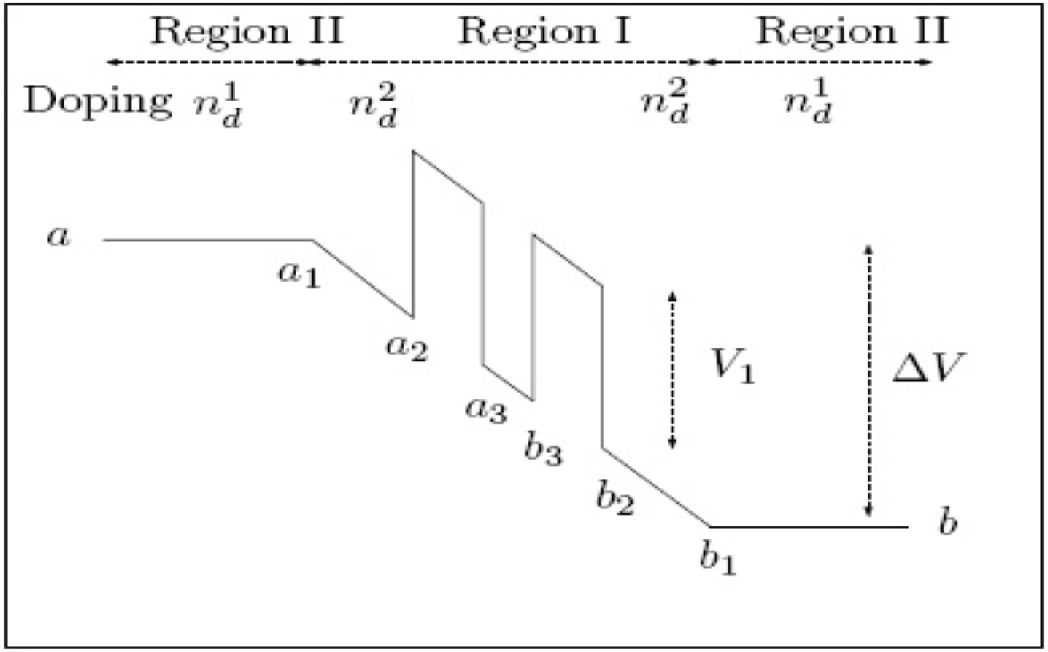

Figure: Schematics of the potential energy in a RTD (*Ben Abdallah & Pinaud, 2006*).

Schrödinger-Poisson problem for RTD:

- **Schrödinger Eq. for wavefunction $\boldsymbol{\varphi_p(x)}$:**

$$\begin{cases} -\dfrac{\hbar^2}{2m}\,\varphi_p''(x) - q\,V(x)\,\varphi_p(x) = E\,\varphi_p(x) \quad \text{on } [a,b], \\ \hbar\,\varphi_p'(a) + ip\,\varphi_p(a) = 2ip, \qquad \hbar\,\varphi_p'(b) = ip_b\,\varphi_p(b). \end{cases}$$

Total electrostatic potential $V = V_e + V_s$

- **Electronic density:**

$$n(x) = \int_{-\infty}^{\infty} g(p)\,\left|\varphi_p\,(x)\right|^2\,dp.$$

- **Poisson Eq. for $\boldsymbol{V_s}$:**

$$\begin{cases} V_s''(x) = \dfrac{q}{\epsilon}\big(n(x) - n_D(x)\big), \\ V_s(a) = V_s(b) = 0. \end{cases}$$

The algorithm for solving the Schrödinger -Poisson problem:

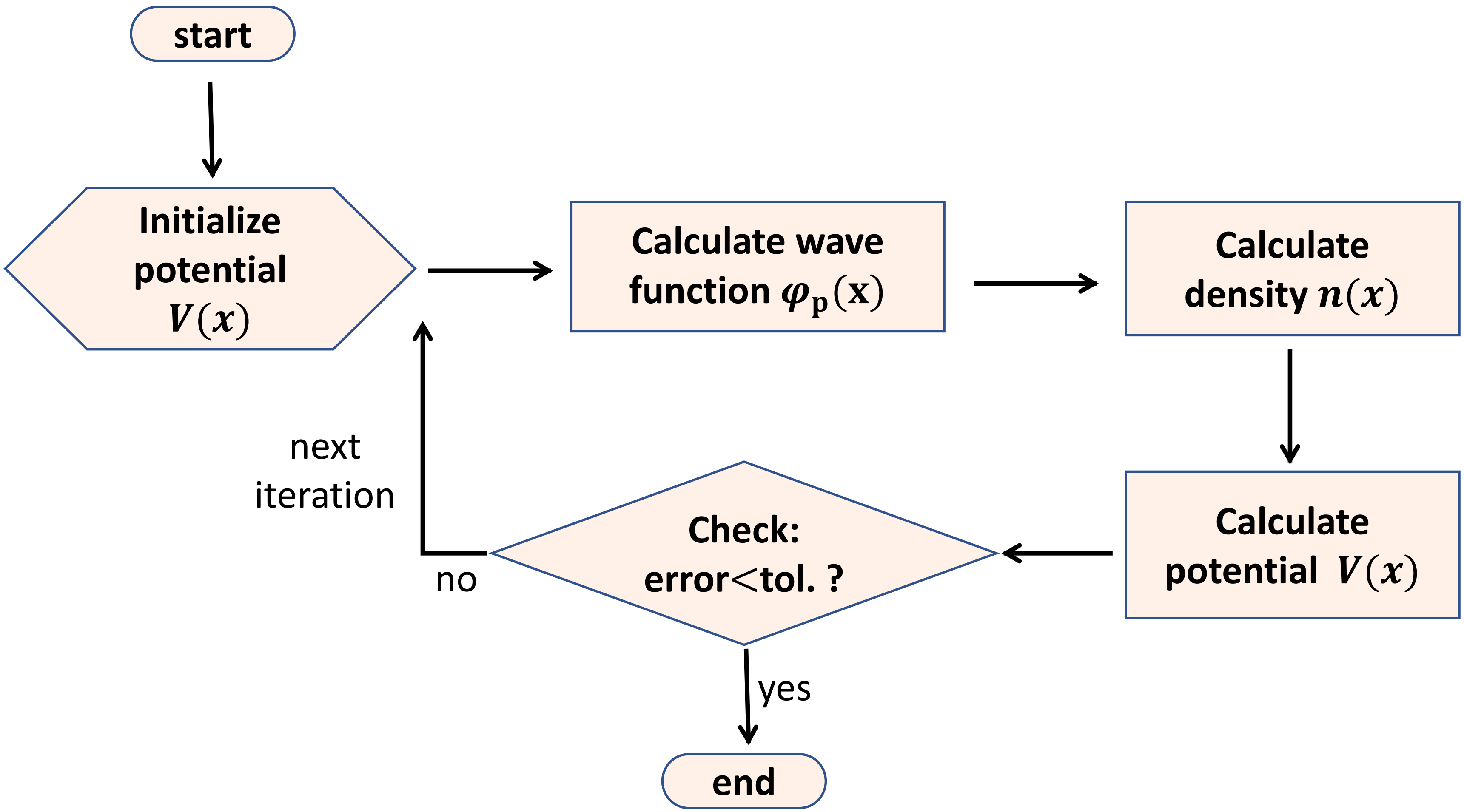

Numerical difficulties:

- Large number of Schrödinger equations to be solved
- Highly oscillating solution for large energy E is large.

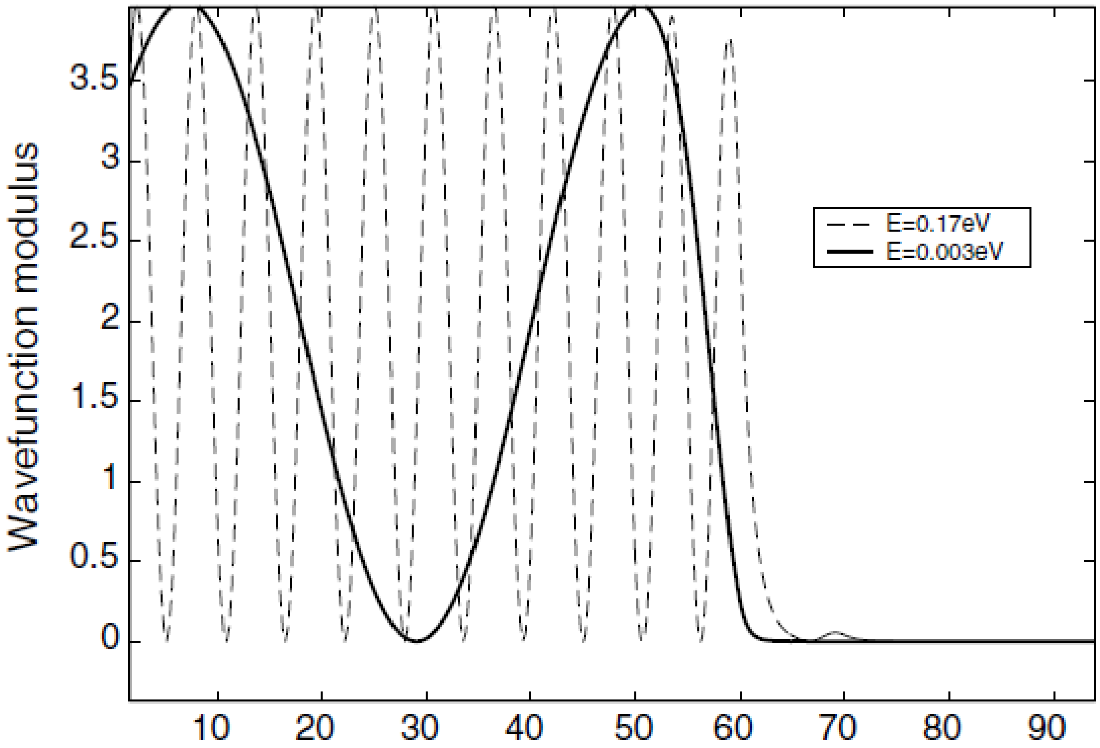

Model problem

Schrödinger Eq. :

$$\begin{cases} -\dfrac{\hbar^2}{2m}\,\varphi_p''(x) - q\,V(x)\,\varphi_p(x) = E\,\varphi_p,(x), & a < x < b \\ \hbar\,\varphi_p'(a) + ip\,\varphi_p(a) = 2ip, \qquad \hbar\,\varphi_p'(b) = ip_b\,\varphi_p(b). & \end{cases}$$

Let $\varepsilon = \frac{\hbar}{\sqrt{2mE}}, f(x) = 1 + \frac{qV(x)}{E}$.

Model problem:

$$\boxed{\begin{cases} -\varepsilon^2 u'' - f(x)u = 0, \qquad a < x < b \\ u'(a) + ik_a u(a) = 2ik_a,\ u'(b) - ik_b u(b) = 0, \end{cases}}$$

where $0 < \varepsilon < 1$, and $f(x)$ is independent of ε.

Assume $f > 0$. The solution is a wave function with **wave number** $\boldsymbol{k(x) = \frac{\sqrt{f(x)}}{\varepsilon}}$.

Standard finite element methods using polynomials require very fine mesh to capture oscillatory solutions.

E.g. LDG using piecewise polynomials of degree 1 and 2 for solving the Schrödinger eqn.

N	P^1				P^2			
	$\varepsilon = 10^{-2}$		$\varepsilon = 10^{-3}$		$\varepsilon = 10^{-2}$		$\varepsilon = 10^{-3}$	
	Error	Order	Error	Order	Error	Order	Error	Order
10	9.53E−01	–	9.51E−01	–	9.47E−01	–	9.51E−01	–
20	9.60E−01	−0.01	9.51E−01	0.00	9.55E−01	−0.01	9.51E−01	0.00
40	9.51E−01	0.01	9.51E−01	0.00	4.46E−01	1.10	9.51E−01	0.00
80	1.17E−00	−0.29	9.51E−01	0.00	3.92E−02	3.51	9.52E−01	0.00
160	7.88E−02	3.89	9.52E−01	0.00	4.42E−03	3.15	9.53E−01	0.00
320	1.42E−02	2.47	9.57E−01	−0.01	5.51E−04	3.00	2.05E−00	−1.11
640	3.49E−03	2.02	2.08E−00	−1.12	6.88E−05	3.00	7.72E−01	1.41

Previous work:

- **Ben Abdallah, Pinaud, Mouis, Negulescu, Arnold, Polizzi (2004-2008, 2011)**

WKB asymptotics: If $E+qV>0$, when $\hbar\to 0$,

$$\varphi(x)\sim\frac{A}{\sqrt{k(x)}}\,e^{iS(x)}+\frac{B}{\sqrt{k(x)}}\,e^{-iS(x)},\quad \text{where } S(x)=\int_{x_0}^{x}k(s)\,ds.$$

Multiscale continuous finite element basis:

$$\tilde{\varphi}(x)=\frac{A_j}{\sqrt{k(x)}}\,e^{i\,S(x)}+\frac{B_j}{\sqrt{k(x)}}\,e^{-i\,S(x)},\ x\in I_j.$$

- **Wang, Shu (2008)**

WKB- local DG method:

$$E^2=\left\{v_h\colon v_h|_{I_j}\in\text{span}\left\{1,\,e^{ik_j(x-x_j)},e^{-ik_j(x-x_j)}\right\},\ j=1,\cdots,N\right\},$$

where $k_j=k(x_j), x_j$ is the middle point of I_j.

Our second-order multiscale DG method

Finite element space:

$$E^1 = \left\{ v_h : v_h \Big|_{I_j} \in \operatorname{span}\left\{ e^{ik_j(x-x_j)}, e^{-ik_j(x-x_j)} \right\}, \qquad j = 1, \cdots, N \right\}$$

Model Eq.: $$-\varepsilon^2 u'' - f(x)u = 0$$

Mixed form:
$$q - \varepsilon u' = 0,$$
$$-\varepsilon q' - f(x)u = 0.$$

DG formulation:

$$\begin{cases} \int_{I_j} q_h \, v \, dx + \int_{I_j} \varepsilon \, u_h v' dx - \varepsilon \, \hat{u}_h v\big|_{x_j}^{x_{j+1}} = 0, \\ \int_{I_j} \varepsilon \, q_h w' dx \; - \varepsilon \, \hat{q}_h w\big|_{x_j}^{x_{j+1}} - \int_{I_j} f(x) u_h w \, dx = 0. \end{cases}$$

Numerical traces:

Interior nodes:
$$\hat{u}_h = u_h^- - i\beta(q_h^- - q_h^+),$$
$$\hat{q}_h = q_h^+ + i\alpha(u_h^- - u_h^+).$$

Boundary nodes:
$$\begin{cases} \widehat{u}_h(a) = (1-\gamma)u_h(a) + i\dfrac{\gamma}{\sqrt{f_a}}q_h(a) + 2\gamma, \\ \widehat{q}_h(a) = \gamma q_h(a) - i(1-\gamma)\sqrt{f_a}\,u_h(a) + 2i\,(1-\gamma)\sqrt{f_a}, \end{cases}$$
$$\begin{cases} \widehat{u}_h(b) = (1-\gamma)u_h(b) - i\dfrac{\gamma}{\sqrt{f_b}}q_h(b), \\ \widehat{q}_h(b) = \gamma q_h(b) + i(1-\gamma)\sqrt{f_b}\,u_h(b), \end{cases}$$

which satisfy that

$$\widehat{q}_h(a) + i\sqrt{f_a}\widehat{u}_h(a) = 2i\sqrt{f_a}, \quad \widehat{q}_h(b) - \mathbf{i}\sqrt{f_b}\widehat{u}_h(b) = 0.$$

Error Estimate

In our analysis, we assume that $f \in W^{1,\infty}(\Omega)$ and

$$f(x) \geq \tau > 0 \quad \text{for any } x \in \Omega_h.$$

Theorem: (Dong, Shu, Wang 2016)

Assume that $\alpha > 0, \beta > 0,$ and $0 < \gamma < 1$. For any mesh size $h > 0$, we have

$$\|u - u_h\| \leq C|f|_{1,\infty}\left(\frac{h^2}{\varepsilon} + \frac{h^3}{\varepsilon^2}\right)\|u\|$$

where C is a constant independent of ε and h.

Lemma: (Dong, Shu, Wang 2016)

If a function φ is the solution to the equation

$$-\varepsilon^2\varphi'' - f(x)\varphi = \theta,$$

where $\theta \in L^2(\Omega_{\mathrm{h}})$, Π is the L^2-projection onto E^1, and $\psi = \varepsilon\varphi'$, then on each $I_j \in \Omega_h$, for any $h > 0$, we have

$$\|\varphi - \Pi\varphi\|_{I_j} + \|\psi - \Pi\psi\|_{I_j} \leq C\frac{h}{\varepsilon}(\|\theta\|_{I_j} + h|f|_{W^{1,\infty}(I_j)}\|\phi\|_{I_j})$$

and

$$\|\varphi - \Pi\varphi\|_{\partial I_j} + \|\psi - \Pi\psi\|_{\partial I_j} \leq C\frac{h^{1/2}}{\varepsilon}(\|\theta\|_{I_j} + h|f|_{W^{1,\infty}(I_j)}\|\phi\|_{I_j}),$$

where C is a constant independent of ε and h.

High-order multiscale DG

DG formulation: the same

Numerical traces: the same

Two high-order multiscale approximation spaces:

- $E^{p+2}|_{I_j} = span\left\{e^{\pm ik_j(x-x_j)}, \mathbf{1}, \boldsymbol{x}, \cdots, \boldsymbol{x}^{p}\right\}$ for any $p \geq 0$.
- $T^{2p+1}|_{I_j} = span\left\{e^{\pm ik_j(x-x_j)}, \boldsymbol{e}^{\pm 2ik_j(x-x_j)}, \cdots, \boldsymbol{e}^{\pm(p+1)ik_j(x-x_j)}\right\}$ for any $p \geq 0$.

Remark:

- $E^{p+2}|_{I_j} = E^1|_{I_j} \oplus P^p$, where P^p is the space of polynomials up to degree p on I_j.
  On each element I_j, E^{p+2} has the same number basis functions as P^{p+2}.
- When $p = 0$, $T^{2p+1} = T^1 = E^1$.
  On each element I_j, T^{2p+1} has the same number of basis functions as P^{2p+1}.

Error Estimate

Theorem: (Dong, Wang, submitted)

Suppose u_h and $\tilde{u}_h$ are the solutions of the multiscale DG methods using E^{p+2} and T^{2p+1}, respectively. Assume that $\alpha, \beta > 0$ and $0 < \gamma < 1$.

When h is small enough, for any $p \geq 0$, we have

$$\|u - u_h\| \leq C h^{\min\{s+1, p+3\}} (\|u\|_{s+1} + \|q\|_{s+1}),$$

$$\|u - \tilde{u}_h\| \leq C h^{\min\{s+1, 2p+2\}} (\|u\|_{s+1} + \|q\|_{s+1}),$$

where C is independent of h.

outline

- Model problem
- Multiscale discontinuous Galerkin (DG) methods; error estimates
  - a second-order multiscale DG
  - two classes of higher order multiscale DG
- Numerical results
- Concluding Remarks

Numerical Experiment 1: (Constant f)

We take $\alpha = \beta = 1, \gamma = 0.5,$ and $f(x) = 10.$

Table 1. L^2-errors of multiscale DG methods when $\varepsilon = 0.01$.

N	E^1	E^2	E^3	T^3	T^5
10	6.93E-13	7.05E-13	6.38E-13	6.82E-13	6.69E-13
100	5.92E-13	5.67E-13	5.62E-13	5.74E-13	5.63E-13

Remark: For other values of ε, the results are similar.

Numerical Experiment 2: (Accuracy test)

- Take $f(x) = 2 + \sin x$.
- The reference solution is computed by $MD\text{-}LDG\ P^3$ with $N = 500{,}000$.

For $\varepsilon = 0.01$:

	E^1		E^2		E^3	
N	error	order	error	order	error	order
10	2.56E-02	–	2.54E-02	–	2.22E-02	–
20	7.08E-03	1.85	3.49E-03	1.92	2.56E-03	3.12
40	2.50E-03	1.50	6.19E-04	3.44	6.28E-04	2.03
80	4.37E-04	2.52	1.22E-04	2.35	3.71E-05	4.08
160	7.17E-05	2.61	2.90E-05	2.07	1.45E-06	4.67
320	1.60E-05	2.17	5.43E-06	2.42		
640	3.89E-06	2.04	8.35E-07	2.70		

	T^3		T^5	
N	error	order	error	order
10	2.53E-02	–	2.52E-02	–
20	7.05E-03	1.84	7.14E-03	1.82
40	1.03E-03	2.77	2.95E-04	4.60
60	7.74E-05	6.39	1.36E-05	7.58
80	2.02E-05	4.67	1.86E-06	6.94
100	7.13E-06	4.67		

Comparison of our multiscale DG with the standard DG using polynomial basis for $\varepsilon = 0.01$:

	P^1		P^2		P^3	
N	error	order	error	order	error	order
10	9.53E-01	–	9.47E-01	–	9.48E-01	–
20	9.60E-01	-0.01	9.55E-01	-0.01	1.63E+00	-0.78
40	9.51E-01	0.01	4.46E-01	1.10	7.45E-02	4.45
80	1.17E-00	-0.29	3.92E-02	3.51	4.23E-03	4.14
160	7.88E-02	3.89	4.42E-03	3.15	2.67E-04	3.98

	E^1		E^2		E^3	
N	error	order	error	order	error	order
10	2.56E-02	–	2.54E-02	–	2.22E-02	–
20	7.08E-03	1.85	3.49E-03	1.92	2.56E-03	3.12
40	2.50E-03	1.50	6.19E-04	3.44	6.28E-04	2.03
80	4.37E-04	2.52	1.22E-04	2.35	3.71E-05	4.08
160	7.17E-05	2.61	2.90E-05	2.07	1.45E-06	4.67
320	1.60E-05	2.17	5.43E-06	2.42		
640	3.89E-06	2.04	8.35E-07	2.70		

Comparison of our multiscale DG with the standard DG using polynomial basis for $\varepsilon = 0.01$:

	P^1		P^2		P^3	
N	error	order	error	order	error	order
10	9.53E-01	–	9.47E-01	–	9.48E-01	–
20	9.60E-01	-0.01	9.55E-01	-0.01	1.63E+00	-0.78
40	9.51E-01	0.01	4.46E-01	1.10	7.45E-02	4.45
80	1.17E-00	-0.29	3.92E-02	3.51	4.23E-03	4.14
160	7.88E-02	3.89	4.42E-03	3.15	2.67E-04	3.98

	E^1		E^2		E^3	
N	error	order	error	order	error	order
10	2.56E-02	–	2.54E-02	–	2.22E-02	–
20	7.08E-03	1.85	3.49E-03	1.92	2.56E-03	3.12
40	2.50E-03	1.50	6.19E-04	3.44	6.28E-04	2.03
80	4.37E-04	2.52	1.22E-04	2.35	3.71E-05	4.08
160	7.17E-05	2.61	2.90E-05	2.07	1.45E-06	4.67
320	1.60E-05	2.17	5.43E-06	2.42		
640	3.89E-06	2.04	8.35E-07	2.70		

Numerical Experiment 3: (Application to the RTD model):

- Double barriers of height −0.3v are located at [60, 65] and [70, 75].

$$V(x) = \begin{cases} 0, & x < 60 \\ -0.3, & 60 < x < 65 \\ 0, & 65 < x < 70 \\ -0.3, & 70 < x < 75 \\ 0, & x > 75 \end{cases} .$$

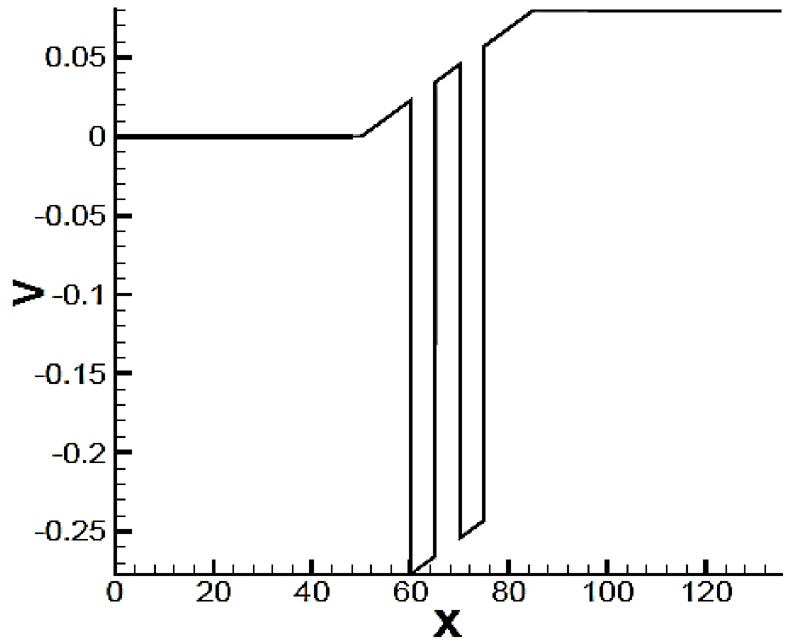

- A bias of 0.08 V is applied.
- $E = 1.11\ eV$.
- Reference solution is computed using MD-LDG P^3 using 13,500 cells.
- 54 uniform cells are used for multiscale DG with E^1, E^2, E^3, T^3, T^5.

Table: L^2-error by multiscale DG for Schrödinger eq. in RTD model

N	E^1	E^2	E^3	T^3	T^5
54	1.54E-05	5.44E-07	2.28E-07	4.63E-06	3.36E-07

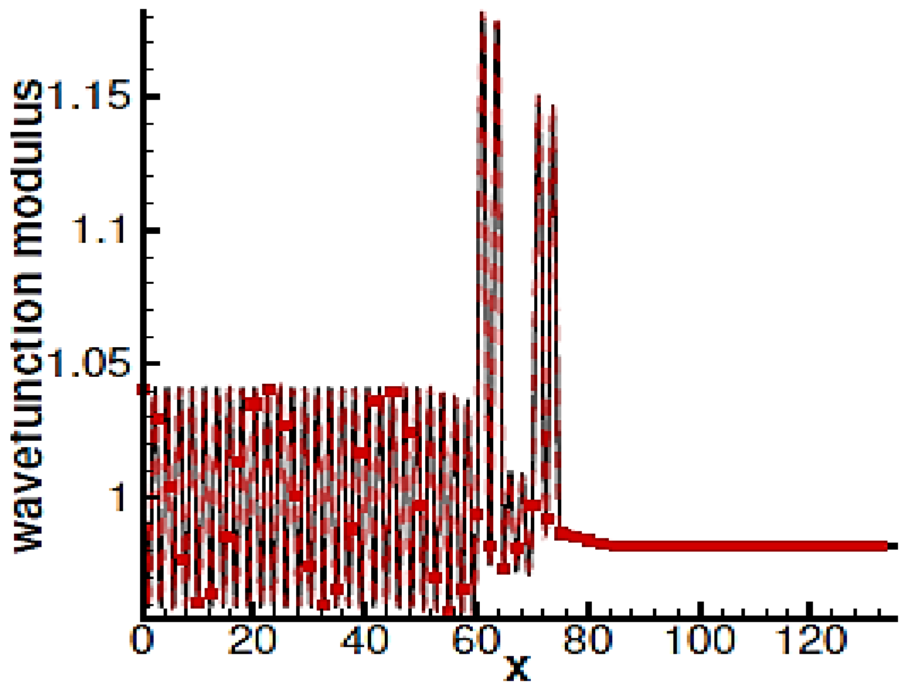

Fig. Wavefunction modulus by the multiscale DG with E^1 space using 54 uniform cells. Solid line: exact solution; dashed line: numerical solution. The graphs for using E^2, E^3, T^3, T^5 are similar.

Conclusions and Future Work:

- When f is constant, the multiscale DG methods can all resolve the exact solution.
- We prove that the multiscale DG method using the E^1 space has optimal convergence rate for any h.
- The high-order multiscale DG methods using E^{p+2} or T^{2p+1} spaces have second-order convergence on coarse meshes and optimal high-order convergence on fine meshes.
- The ongoing work is to generalize the multiscale DG methods to two-dimensional Schrödinger equations.

Thank you!

L^2-errors and orders of accuracy by WKB-LDG in [18] where $\alpha = \beta = \gamma = 0$

N	$\varepsilon = 1$		$\varepsilon = 10^{-2}$		$\varepsilon = 10^{-3}$		$\varepsilon = 10^{-4}$	
	Error	Order	Error	Order	Error	Order	Error	Order
10	4.02E−06	–	2.54E−2	–	2.52E−01	–	1.58E−00	–
20	5.70E−07	2.82	5.70E−02	$\boxed{-1.17}$	6.58E−02	1.94	6.21E−01	1.35
40	–	–	5.51E−04	6.69	1.58E−02	2.06	1.58E−01	1.97
80	–	–	7.43E−05	2.89	3.89E−03	2.02	3.96E−02	2.00
160	–	–	9.63E−06	2.95	7.56E−03	$\boxed{-0.96}$	9.90E−03	2.00
320	–	–	1.21E−06	2.99	1.16E−04	6.03	3.68E−03	1.43
640	–	–	1.55E−07	2.97	1.41E−05	3.04	7.13E−04	2.37